THE JOURNAL OF BIOLOGICAL CHEMISTRY VOL. 283, NO. 13, pp. 8643–8653, March 28, 2008

Correlation of the Tight Junction-like Distribution of Claudin-1 to the Cellular Tropism of Hepatitis C Virus*[S]

Received for publication, December 3, 2007, and in revised form, January 22, 2008 Published, JBC Papers in Press, January 22, 2008, DOI 10.1074/jbc.M709824200

Wei Yang[‡], Chao Qiu[‡1], Nabanita Biswas[‡], Jing Jin[‡§], Simon C. Watkins[¶], Ronald C. Montelaro[‡§], Carolyn B. Coyne[¶], and Tianyi Wang[‡2]

From the Departments of [‡]Infectious Diseases and Microbiology, [§]Microbiology and Molecular Genetics, and [¶]Cell Biology and Physiology, University of Pittsburgh, Pittsburgh, Pennsylvania 15261

Claudin-1 (CLDN1), a tight junction (TJ) protein, has recently been identified as an entry co-receptor for hepatitis C virus (HCV). Ectopic expression of CLDN1 rendered several non-hepatic cell lines permissive to HCV infection. However, little is known about the mechanism by which CLDN1 mediates HCV entry. It is believed that an additional entry receptor(s) is required because ectopic expression of CLDN1 in both HeLa and NIH3T3 cells failed to confer susceptibility to viral infection. Here we found that CLDN1 was co-immunoprecipitated with both HCV envelope proteins when expressed in 293T cells. Results from biomolecular fluorescence complementation assay showed that overexpressed CLDN1 also formed complexes with CD81 and low density lipoprotein receptor. Subsequent imaging analysis revealed that CLDN1 was highly enriched at sites of cell-cell contact in permissive cell lines, co-localizing with the TJ marker, ZO-1. However, in both HeLa and NIH3T3 cells the ectopically expressed CLDN1 appeared to reside predominantly in intracellular vesicles. The CLDN1-CD81 complex formed in HeLa cells was also exclusively distributed intracellularly, co-localizing with EEA1, an early endosomal marker. Correspondingly, transepithelial electric resistance, obtained from the naturally susceptible human liver cell line, Huh7, was much higher than that of the HeLa-CLDN1 cell line, suggesting that Huh7 is likely to form functional tight junctions. Finally, the disruption of TJ-enriched CLDN1 by tumor necrosis factor-α treatment markedly reduced the susceptibility of Huh7.5.1 cells to HCV infection. Our results suggest that the specific localization pattern of CLDN1 may be crucial in the regulation of HCV cellular tropism.

Hepatitis C virus (HCV),[3] a major human pathogen, specifically infects hepatocytes. In nature, the virus may exist in several forms: enveloped lipoprotein-free virus, enveloped lipoprotein-associated virus, non-enveloped lipoprotein-free virus, and non-enveloped lipoprotein-associated virus (1). While the nature of these different forms remains elusive, they may infect cells via different means (1). Importantly, pseudoviral particles that consist of an HIV core and HCV E1 and E2 (*i.e.* HCVpp) have been found to strictly infect human hepatocytes and a few hepatoma-derived cell lines (2–4). HCVpp most likely resembles enveloped lipoprotein-free viruses whose entry is dependent upon two of the HCV envelope proteins, E1 and E2 (5–9). A plethora of evidence that has been accumulated from studies employing HCVpp has allowed for a proposed model of HCV entry: HCV attaches to hepatocytes via specific receptor(s) followed by clathrin-dependent internalization (endocytosis) (10, 11). Internalized virions then traffic to early endosomes where the virion envelope proteins undergo conformational changes and then fuse with the cellular membrane for viral entry (4, 12). In numerous attempts to identify an HCV entry receptor(s), both human tetraspanin CD81 and the human scavenger receptor, SR-BI, were isolated in screens based on sE2 binding (9, 13, 14). Intensive studies using HCVpp and the recently developed cell culture-grown HCV system (HCVcc) have now firmly established the necessary roles of CD81 and SR-BI in HCV entry (2, 3, 15–18).

Most recently, Evans *et al.* (19) have identified a tight junction (TJ) protein, Claudin-1 (CLDN1), as the third entry co-receptor for HCV. Like CD81, CLDN1 spans the plasma membrane four times and is a component of the tight junction barrier that restricts the free exchange of ions and aqueous molecules between cells (20, 21). It was shown that CLDN1 is required for HCV infection of human hepatoma cell lines and was the first factor to confer susceptibility to HCV when ectopically expressed in non-hepatic cell types (19). Discrete residues within the first extracellular loop (EL1) of CLDN1, but not the protein interaction motifs within the intracellular domains, are required for HCV entry. While the precise role of CLDN1 in

* This work was supported in part by National Institutes of Health Grant 1R21AI068784-01A1 (to T. W.) and University of Pittsburgh Central Research Development Funds (to T. W.). The costs of publication of this article were defrayed in part by the payment of page charges. This article must therefore be hereby marked "*advertisement*" in accordance with 18 U.S.C. Section 1734 solely to indicate this fact.

[S] The on-line version of this article (available at http://www.jbc.org) contains supplemental Figs. S1–S4.

[1] Present address: Laboratoire d'Immunologie, Centre de Recherche du Centre Hospitalier de l'Université de Montréal (CR-CHUM) Saint-Luc, 264 Rene Levesque Est, Montréal, Québec H2X1P1, Canada.

[2] To whom correspondence should be addressed: Dept. of Infectious Diseases and Microbiology, Graduate School of Public Health, 130 DeSoto St., Pittsburgh, PA 15261. Tel.: 412-383-9916; Fax: 412-383-8926; E-mail: tywang@pitt.edu.

[3] The abbreviations used are: HCV, hepatitis C virus; HCVpp, HIV particles pseudotyped with HCV envelope proteins; VSVpp, HIV particles pseudotyped with vesicular stomatitis virus envelope protein G; HCVcc, cell culture-grown HCV; CLDN1, Claudin-1; BiFC, biomolecular fluorescence complementation assay; TNF, tumor necrosis factor; PBS, phosphate-buffered saline; GFP, green fluorescent protein; IFN, interferon; TJ, tight junction; FITC, fluorescein isothiocyanate; TER, transepithelial electric resistance; LDLR, low density lipoprotein receptor.

HCV entry remains unclear, it was shown to facilitate fusion between virions and cell membranes in a fusion assay (19), indicating that it is a critical component for entry. However, several cell lines remained resistant to HCVpp infection, even upon the ectopic expression of CLDN1. It is therefore reasonable to assume that an additional factor(s) is required for viral entry.

In an attempt to define the role of CLDN1 in HCV entry, we performed co-immunoprecipitation studies and demonstrated that overexpressed CLDN1 could interact with HCV E1 and E2, CD81, and the low density lipoprotein receptor (LDLR). We then fortuitously found that the subcellular distribution of CLDN1 correlated with the permissiveness of the cells to HCVpp infection. Specifically, ectopically expressed CLDN1 in non-permissive lines was localized predominantly within intracellular vesicles, whereas in permissive lines, it was enriched at sites of cell-cell contact. Huh7 cells displayed a considerably high transepithelial electric resistance compared with HeLa-CLDN1 cells, indicating that they form functional TJs that prohibit free ion diffusion. Endogenous CLDN1 also co-localized with the TJ marker, ZO-1, at cell-cell contacts in Huh7 cells, suggesting that these cells form TJs. Finally, tumor necrosis factor α (TNF-α) treatment disrupted the cell surface expression of CLDN1 in the Huh7.5.1 cell line; as a result, treated cells showed decreased susceptibility to HCVpp infection. These results suggest that cell type-specific CLDN1 localization may be a novel mechanism by which the HCV cellular tropism is controlled.

EXPERIMENTAL PROCEDURES

Cell Lines and Reagents—The human kidney epithelial cell line HEK293T (CRL-11268), the human intestinal epithelial cell line Caco-2 (HTB-37), mouse fibroblast NIH3T3 cells (CRL-1658), and the human lung cancer cell line A549 (CCL-185) were purchased from The American Type Culture Collection (ATCC). The human osteosarcoma cell line Ghost and the human cervical carcinoma cell line HeLa were both obtained through the NIAID AIDS research and reference program. HepG2 cells were provided by Dr. QingDe Wang (University of Pittsburgh Cancer Institute). The human liver cell line Huh7 was obtained from Apath Inc., with the permission of Dr. Charles Rice (Rockefeller University). The Huh7.5.1 line generated from a cured HCV replicon cell line was provided by Dr. Francis Chisari (Scripps Research Institute). A Huh7 cell line stably producing JFH1 HCVcc was a generous gift from Dr. G. Luo (University of Kentucky) (22). All cell lines except A549 were maintained in Dulbecco's modified Eagle's medium supplemented with 5% penicillin and streptomycin, 1% NEAA, and 10% fetal bovine serum (Hyclone). The A549 cell line was maintained in F12K media supplemented with 10% fetal bovine serum and 5% penicillin and streptomycin. Antibodies were obtained from Dr. Harry Greenberg (HCV E1, clone A4), Dr. Jean Dubuisson (HCV E2, clones H47, H52, H53), Zymed Laboratories Inc. (anti-CLDN1, clones 2H10D10 and JAY.8, and anti-ZO-1, clone ZO1-1A12), BD Bioscience (monoclonal anti-EEA1), and Sigma (anti-FLAG M2 and β-actin).

DNA Constructs—Full-length human CLDN1, CD81, LDLR, HCV E1, E2, and MLV envelope protein (MLV Env) were cloned into the XbaI/NotI sites of the pcDNA3-VN and pcDNA3-VC plasmids to produce fusions to N-terminal residues 1–172 (VN), or C-terminal residues 155–238 (VC) of the Venus protein, leaving the VN- or VC-tagged to the C terminus of the target proteins. hCLDN1, FLAG-CLDN1, and CD81 were also cloned between the BglII/XhoI sites of the pMIR-DFT plasmid for expression. CLDN1-EGFP was generated by inserting the hCLDN1 gene between the BglII/SalI sites of the pEGFP-N2 vector (Clontech). Detailed plasmid maps are available upon request. pCMV E1 and E2 were provided by Dr. Charles Rice (Rockefeller University) expressing full-length genotype 1a (H77) HCV E1 and E2 (4).

Production of HCVpp—To produce the pseudovirus, HEK293T cells were seeded 1 day prior to transfection at 2.5×10^6 cells in a 10-cm plate in 10 ml of Dulbecco's modified Eagle's medium containing 10% fetal bovine serum. The next day, cells were transfected using Lipofectamine 2000 (Invitrogen) or the standard calcium phosphate transfection method. The DNA transfection mixture (1 ml) was composed of 10 μg of pNL-4.3-Luc-E-R- (obtained through the NIAID AIDS research and reagent program), 10 μg of phCMV-HCV E1E2 (a generous gift from Dr. Cosset, INSERM, France), or 3 μg of pHEF-VSV-G (expressing the VSV-G Env protein). pNL-4.3-Luc-E-R- expresses all the HIV proteins except Env, Vpr, and Nef. Two frameshift mutations were introduced into the Env- and Vpr-coding regions and the firefly luciferase gene was inserted in-frame immediately downstream of the start codon of the Nef gene. As a result, the produced pseudovirus is infectious for only one round. In our study, HCVpp and VSVpp represent lentivirus particles pseudotyped with HCV E1 and E2 glycoproteins or with VSV-G glycoprotein, respectively. A non-enveloped lentivirus particle (Bald virus) was also generated as the negative control. To make this particle, the amount of envelope-encoding plasmid was replaced by the same amount of pcDNA3 empty plasmid. Sixteen hours after transfection, media was replaced; supernatants containing HCVpp were typically harvested 36–48 h after transfection and then filtered through a 0.22-μm syringe filter. Because HIV viral-like particles can be formed and released even in the absence of the Env protein, the level of p24 in the supernatant is not an accurate indicator of HCVpp viral titer. We therefore determined viral titer using an end point titration assay; infection unit/ml (international units/ml) is used to represent the titer of HCVpp. The typical viral titer for HCVpp using the pNL4.3-Luc-E-R- construct is between 4×10^3 and 4×10^4 international units/ml.

HCVpp Infection Assay—To conduct the infection assay, Huh 7 or other cell lines were seeded in a 24-well plate at a density of 1×10^5 cells/well 1 day prior to transduction. The next day, 500 μl of supernatant containing HCVpp or VSVpp or Bald virus was added into each well in the presence of 8 μg/ml polybrene and 10 μl of 2 M HEPES (pH 7.55) and centrifuged in a table-top centrifuge machine (2500 rpm, 30 °C, 90 min). Cells were washed twice in 500 μl of PBS and then 500 μl of fresh media was added into each well. Thirty-six hours after transduction, cells were lysed in 100 μl of passive lysis buffer and 20–50-μl lysate was incubated with 100 μl of luciferase assay buffer according to the manufacturer's instructions (Promega luciferase assay kit). We used a Veritas luminometer and typically obtained counts ranging from 5000 to 100,000 following

this protocol. The background signal from a blank well is usually less than 100 counts.

Western Blotting and Immunoprecipitation—For cell lysate preparation, monolayer cells were lysed with radioimmune precipitation assay buffer (50 mM Tris-HCl, pH 7.5, 150 mM NaCl, 0.5% Nonidet P40, 50 mM NaF, 1 mM Na_3VO_4, 5 mM β-glycerophosphate, 1 mM dithiothreitol, 1 mM phenylmethylsulfonyl fluoride) supplemented with a protease inhibitor mixture (Sigma) on ice. The lysate was cleared by centrifuging at 14,000 × *g* for 20 min. Boiled samples in 2× SDS loading buffer were loaded onto a 10–12% polyacrylamide gel. After electrophoresis, the separated proteins were transferred onto a nitrocellulose membrane (Bio-Rad). The resulting blots were blocked in 10% milk for 1 h, and then incubated with primary antibody overnight at 4 °C. The secondary antibody used in the immunoblot was a 1:2000 dilution of HRP-linked anti-IgG. The ECL reagent (Amersham Biosciences, Piscataway, NJ) was used as the substrate for detection. For immunoprecipitation-coupled Western blotting, the cleared cell lysates were immunoprecipitated with anti-FLAG M2 affinity resin (Sigma) and washed with lysis buffer. Eluted samples were separated by 12% SDS-PAGE and immunoblotted with anti-E1, -E2, and -FLAG antibodies.

HCVcc Production—To produce high titer infectious HCV virus (JFH1 strain), we first collected virus secreted by a Huh 7-stable cell line. The HCV produced by this line was then used to infect a human liver cell line (Huh7.5.1) according to a published procedure (23). On day 7, media was collected containing high-titer viruses. For long-term storage, viruses were aliquoted and stored at −80 °C. This step was shown not to decrease virus infectivity even after three freeze-thaw cycles (17). To determine the viral titer, Huh-7.5.1 cells were seeded on coverslips in 24-well plates at 5×10^4 cells/well. Medium containing HCV was serially diluted 2-fold in complete growth medium and used to infect the seeded cells (3–4 wells per dilution). Forty-eight hours following infection, culture media were aspirated and cells were fixed in 100 μl of 2% paraformaldehyde for 30 min at room temperature. Fixed cells were permeabilized in PBS containing 0.2% Triton-X 100 for 30 min. To stain the cells, a 1:400 (2.5 μg/ml) dilution of monoclonal antibody against the HCV core protein (ABR affinity bioreagent, clone C7–50) was used, and the incubation was carried out at room temperature for 2 h. As a negative control, purified normal mouse IgG1 (Santa Cruz Biotechnology) was included as a primary antibody. After incubation, the antibody solution was discarded and cells were washed three times with 200 μl of PBS followed by an incubation with 50 μl of appropriately diluted FITC-conjugated secondary antibody (1:1,000 dilution) (Santa Cruz Biotechnology) for 1 h at 37 °C. Subsequently, secondary antibody was removed and the cells were washed three times with PBS. The coverslips were then mounted on slides and counterstained with DAPI at a 1:2,000 dilution. Images were obtained by an Olympus Provis II fluorescence microscope. When nearly 100% of the cells were positive for core staining, we then calculated the viral titer as international unit/ml. Our method typically yielded viral titers ranging from 10^5 to 10^6 international units/ml.

Immunofluorescence Staining and Confocal Microscopy—Transfected or infected cells were fixed in 2% paraformaldehyde (30 min, room temperature). Cells were then permeabilized with 0.2% (v/v) Triton X-100 in PBS three times (PBST; 10 min, room temperature), blocked in 0.3% (w/v) bovine serum albumin in PBS (1 h, room temperature), and incubated in PBS (1 h, room temperature) with appropriately diluted primary antibodies against CLDN1 (1:80), HCVE2 (clone H47) (1:100), and EEA1 (1:500). Samples were washed in PBS and subsequently incubated with either FITC- or rhodamine-conjugated secondary antibodies diluted in PBS (1:100) according to the manufacturer's instructions (Santa Cruz Biotechnology). Samples were mounted on slides and sealed with nail polish. Images were captured by a Leica TCS-SL confocal microscope, edited using Metamorph, and assembled using Photoshop CS (Adobe). In most studies, the nucleus was stained with Draq5 (Biostatus).

Biomolecular Fluorescence Complementation Assay (BiFC)—We adopted a protocol developed by others (24) for BiFC assays. Briefly, DNA plasmids were incubated with Lipofectamine 2000 (Invitrogen) and transiently transfected into cells preseeded on a 24-well plate. On the day of transfection, the cell density was ~50% confluent. The total amount of DNA plasmids was maintained at 0.25 μg as this amount of DNA was determined previously to yield the highest ratio of BiFC signal over background (24). Twenty-four hours after transfection, cells were fixed and co-stained for other markers when necessary. Samples were then analyzed by either immunofluorescence or confocal microscopy using the FITC filter setting. To quantify the percentage of positive cells, cells were resuspended in PBS (without fixation) and directly analyzed by flow cytometry.

Transepithelial Electric Resistance Measurement—1000 Huh7, Caco-2, and Hela-CLDN1 cells were seeded on a 24-well transwell plate (Corning, 6.5-mm membrane diameter, 0.4-μm pore size). Cells that were resuspended in 0.2 ml of medium were added to the upper chamber, and 0.5 ml of medium was added to the lower chamber in triplicate. Resistance was measured daily for 6 days using an epithelial voltohmmeter (EVOM, World Precision Instruments, Sarasota, FL). A blank well with no cells was maintained, and the average resistance from the blank was subtracted from the sample. Resistance (*R*) per unit area was calculated as $(R_{\text{sample}} - R_{\text{blank}}) \times 0.33\ \text{cm}^2$.

Flow Cytometric Analysis—GFP-positive cells or cells stained with antibodies specific for CD81 or HCVE2 were analyzed on a Coulter XL flow cytometer. Acquired data were analyzed and plotted using WinMDI 2.9 software.

RESULTS

Interactions between CLDN1 and HCV Glycoproteins—Although CLDN1 was suggested as an entry co-receptor for HCV, little is known about the interactions between CLDN1 and HCV envelope proteins (E1 and E2). We therefore performed co-immunoprecipitation experiments and found that FLAG-CLDN1 could pull down HCV E1 and E2 when E1 and E2 were co-expressed in 293T cells from the same plasmid (Fig. 1*A*). Because E1 and E2 are known to dimerize (5, 25), we next expressed E1 and E2 separately in 293T cells and found that both E1 and E2, but not the negative control PLIC-1, could be independently precipitated with FLAG-CLDN1 (Fig. 1*B*). Furthermore, overexpressed HCV E2 partially co-localized with

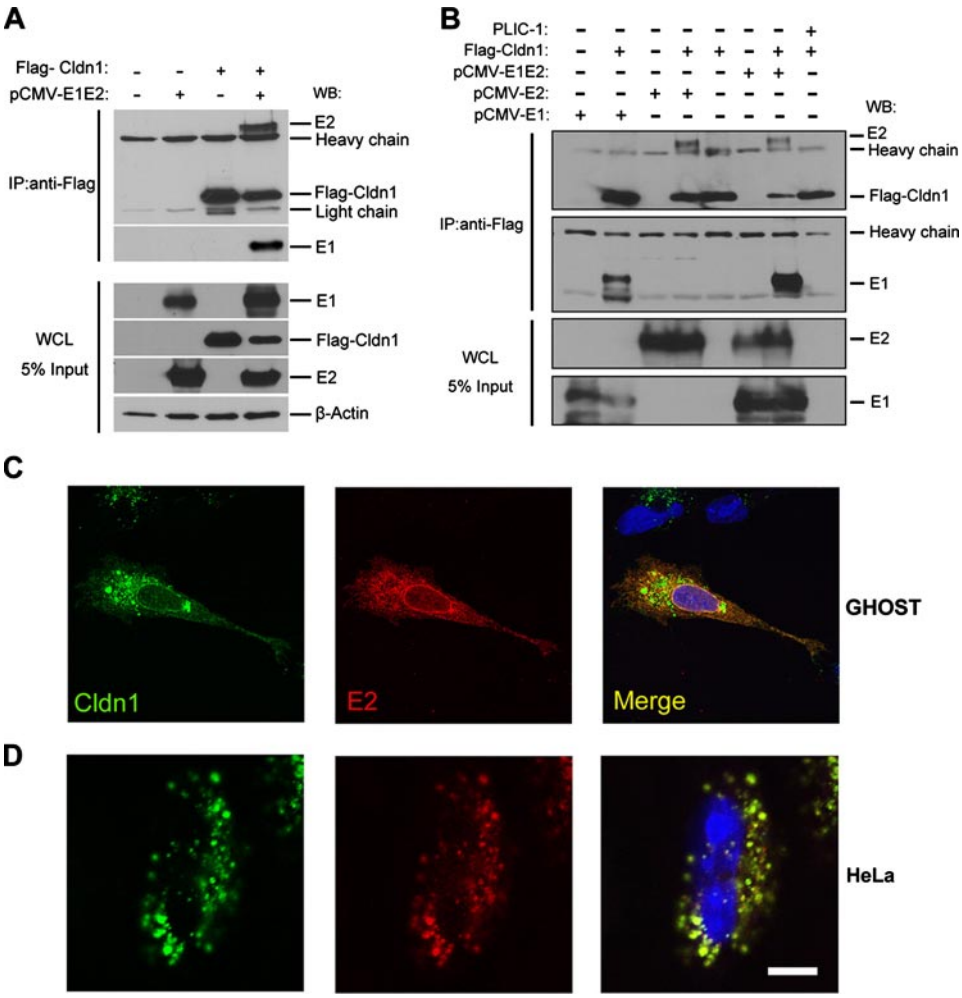

FIGURE 1. **Co-immunoprecipitation and co-localization of CLDN1 and HCV glycoproteins.** *A*, pCMV-E1-E2 plasmid expressing HCV glycoproteins E1 and E2 was transiently transfected into 293T cells with or without the FLAG-CLDN1-expressing plasmid. *Upper panel*, cell lysates containing equivalent amounts of proteins were subjected to immunoprecipitation (*IP*) with an anti-FLAG antibody followed by Western analysis with anti-E1, anti-E2, and anti-FLAG antibodies. *Lower panel*, five percent of the initial whole cell lysates (*WCL*) were analyzed by Western blot for E1, E2, FLAG-CLDN1, and β-actin expression. *B*, same as in *A* except that the construct expressing either E1 or E2 was transfected. A plasmid expressing HA-PLIC-1 (protein linking IAP to cytoskeleton 1) was used as a negative control as we could not detect any HA-PLIC-1 in the pull-downed product (image not shown here). *C*, co-localization of CLDN1 and HCV E2. GHOST cells were co-transfected with plasmids encoding CLDN1-EGFP and E1E2. Twenty-four hours after transfection, cells were fixed and stained with anti-E2 antibody. *D*, same as in *C* except HeLa cells were transfected (*scale bar*, 8 μm).

CLDN1 in vesicular-like structures in both Ghost and HeLa cells (Fig. 1, *C* and *D*). These results suggest that in overexpression systems, CLDN1 is able to interact with both HCV glycoproteins, which is in sharp contrast with CD81 and SR-BI, both of which only interact with E2 (13, 14, 26). Ghost and HeLa cells were chosen for these studies because of their suitable morphology (considerable size of cytoplasm) and relatively high transfection efficiency compared with the human hepatoma cell line Huh7. It should be noted that neither of these lines express endogenous CLDN1 (supplemental Fig. S1, *A* and *B*). Ectopic expression of CLDN1 rendered Ghost but not HeLa cells susceptible to HCVpp infection (supplemental Fig. S1*C*). FLAG-CLDN1 and other tagged proteins used in this study were tested to be functional in infection assays (supplemental Fig. S1*D*).

Association of CLDN1 with CD81 and LDLR—To study the interactions between CLDN1 and other HCV receptors, such as CD81 and LDLR, we utilized a novel approach, the BiFC assay (Fig. 2*A*). In a standard BiFC assay, a fluorescent protein gene is divided into N-terminal and C-terminal segments. Separately, the encoded fragments are unable to fluoresce; however, co-expression of interacting proteins individually fused to these fragments generates detectable fluorescence signal when the two fluorescent protein fragments are placed in close proximity (less than 15 nm). The BiFC assay has been used previously to demonstrate co-assembly of HIV-1 and HIV-2 Gag 319 (27). We prepared a panel of constructs expressing fusion proteins with the optimized N- (VN) and C- (VC) terminal fragments of the Venus fluorescence protein for BiFC assay. One of the advantages of BiFC assay over the regular co-staining method is that the signal can be easily quantified by flow cytometry (Fig. 2*B*). In summary, CLDN1 formed a BiFC complex with HCVE1, E2, CD81, and LDLR, but not with the MLV Env protein. Similar observations could be repeated in the Huh7 cell line despite lower transfection efficiency (data not shown). By contrast, CD81 could only complex with HCV E2 but not E1, which is consistent with a previous report (26). Together, these results confirmed our co-immunoprecipitation studies. Because the addition of VN or VC might disrupt the function of CLDN1, we monitored the expression level of the BiFC constructs by Western analysis and found that they expressed well (Fig. 2*C*). Subsequently, we tested whether these BiFC constructs could mediate HCVpp entry. VN- or VC-fused CLDN1, but not CD81, were able to mediate efficient HCVpp entry into 293T cells (Fig. 2*D* and supplemental Fig. S1*C*). Tagged CD81 was able to render HepG2 cells permissive to HCVpp infection (supplemental Fig. S2*A*) and could be displayed on the cell surface (supplemental Fig. S2*B*) as well; suggesting that the addition of the tag was unlikely to disrupt CD81 function.

HCV entry into target cells is a low pH-dependent process, presumably requiring receptor-mediated endocytosis (10, 12). We sought to examine the subcellular localization of the CLDN1-CD81 and CLDN1-LDLR BiFC complexes by confocal microscopy. It appeared that CLDN1-CD81 and CLDN1-LDLR interactions occurred both on plasma membranes as well as

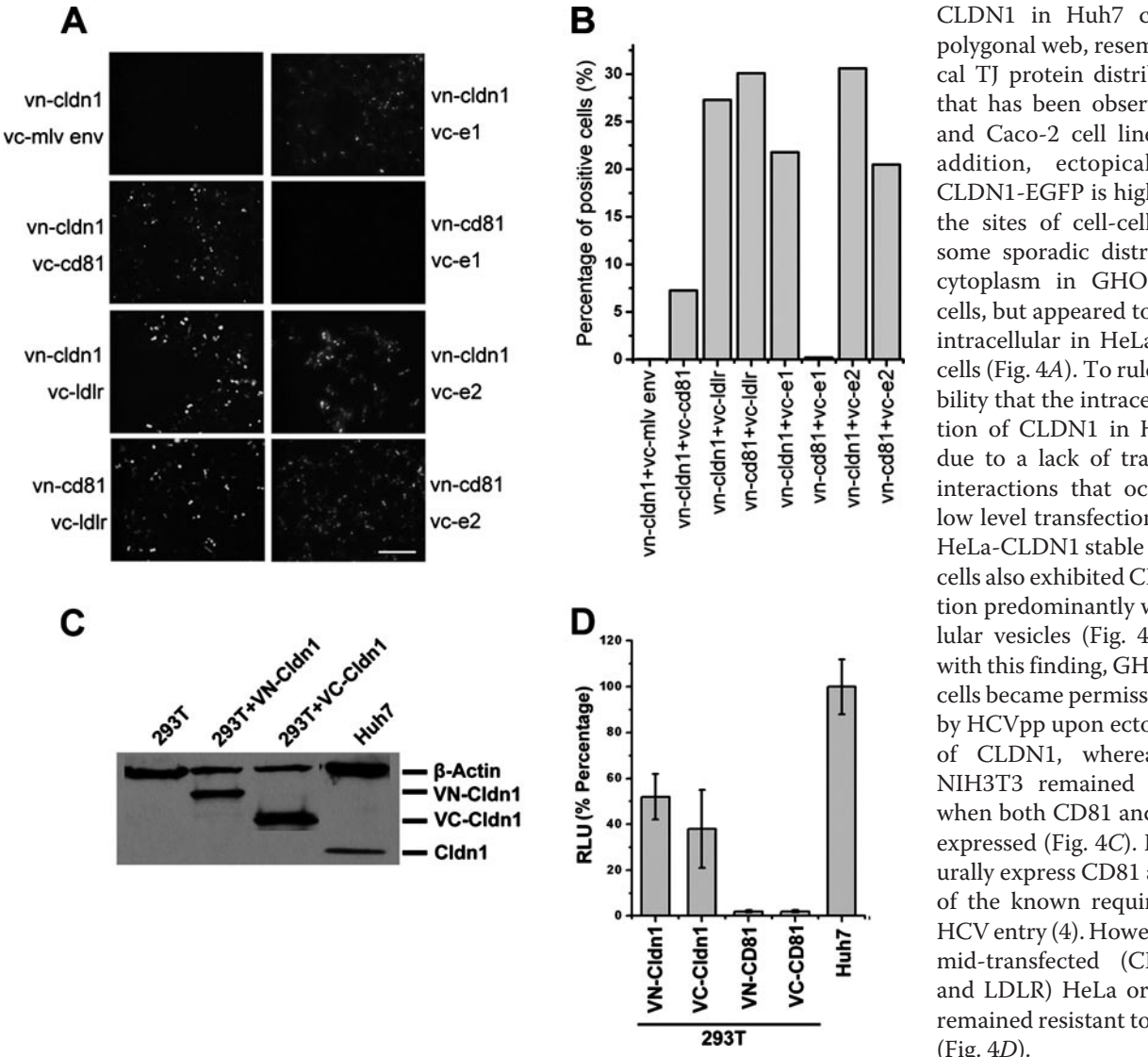

FIGURE 2. **Characterization of the interactions between CLDN1, HCV glycoproteins, and other potential co-receptors by BiFC assay.** *A*, indicated combinations of VN or VC fusion constructs were transfected into 293T cells. Representative images were captured at 24-h post-transfection (*scale bar*, 100 μm) on an Olympus Provis II fluorescence microscope. Quantification of Venus-positive cells was performed by flow cytometry. *B* and *C*, ectopic expression of VN-CLDN1, VC-CLDN1 in 293T cells, and endogenous CLDN1 in Huh7 cells were evaluated by Western blot using an anti-CLDN1 monoclonal antibody. Detection of β-actin was indicative of protein loading. *D*, 293T cells were transfected with the indicated constructs. Twenty-four hours after transfection, cells were spin-infected with HCVpp and cultured for an additional 2 days prior to luciferase assay.

intracellularly in both GHOST (Fig. 3, *A* and *B*) and Huh 7 cell lines (date not shown). The intracellular portion of the formed complex strongly co-localized with early endosome antigen-1 (EEA1), an early endosomal marker. Interestingly, in HeLa cells, the CLDN1-CD81 complex was exclusively concentrated in the cytoplasm and co-localized with EEA1 (Fig. 3*C*). However, the CLDN1-LDLR interaction did not co-localize with EEA1 at all (Fig. 3*D*).

Subcellular Localization of CLDN1 and Cellular Permissiveness to HCVpp—Based on the above observations, we suspected that CLDN1 may be distributed differently among different cell types and the location of CLDN1 may be important in determining its capability in the mediation of viral entry. To test this hypothesis, we investigated the cellular distribution of CLDN1 in various cell lines. Imaging results revealed that endogenous CLDN1 in Huh7 cells formed a polygonal web, resembling the typical TJ protein distribution pattern that has been observed in MDCK and Caco-2 cell lines (28, 29). In addition, ectopically expressed CLDN1-EGFP is highly enriched at the sites of cell-cell contact with some sporadic distribution in the cytoplasm in GHOST and 293T cells, but appeared to be exclusively intracellular in HeLa and NIH3T3 cells (Fig. 4*A*). To rule out the possibility that the intracellular distribution of CLDN1 in HeLa cells was due to a lack of trans-homophilic interactions that occurred due to low level transfection, we created a HeLa-CLDN1 stable cell line. Stable cells also exhibited CLDN1 localization predominantly within intracellular vesicles (Fig. 4*B*). Consistent with this finding, GHOST and 293T cells became permissive to infection by HCVpp upon ectopic expression of CLDN1, whereas HeLa and NIH3T3 remained resistant even when both CD81 and CLDN1 were expressed (Fig. 4*C*). HeLa cells naturally express CD81 and SR-BI, two of the known required factors for HCV entry (4). However, triple plasmid-transfected (CLDN1, CD81, and LDLR) HeLa or NIH3T3 cells remained resistant to such infection (Fig. 4*D*).

We subsequently screened non-hepatic cell lines for CLDN1 expression on plasma membranes and for expression of both CD81 and SR-BI. The human pulmonary epithelial cell line A549 fulfilled our criteria because it expressed both CLDN1 at cell-cell contacts (Fig. 5*A*) and endogenous CD81 (Fig. 5*B*). It also weakly expressed SR-BI (30). Indeed, this line could be infected by HCVpp, albeit, at much lower efficiency compared with Huh7. However, this low infectivity is possibly due to the poor replication of the HIV core protein in A549 cells since VSVpp infection also resulted in an approximate 30-fold decrease in infectivity compared with that in Huh7 cells (Fig. 5*C*). The human intestinal epithelial line Caco-2 was also permissive to HCVpp and expressed all three known HCV receptors (Ref. 31 and supplemental Fig. S3*A*). In contrast, the HeLa-CLDN1 stable line remained resistant to infection (supplemental Fig. S3*B*).

Formation of Tight Junctions in Huh7 Cells—The enrichment of CLDN1 at cell-cell contacts in permissive cell lines is reminiscent of the classical distribution pattern of a TJ-associated

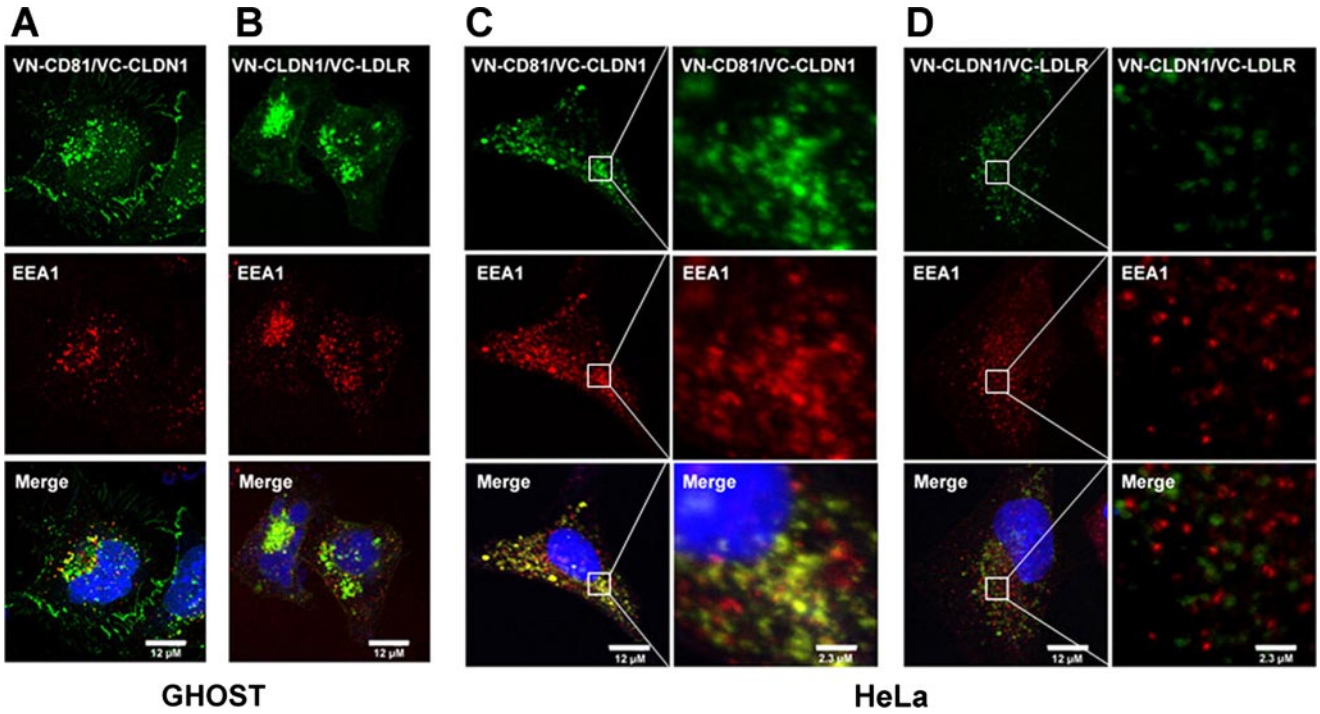

FIGURE 3. **Localization of CLDN1-CD81 and CLDN1-LDLR BiFC complexes.** 0.125 μg of each BiFC construct was transfected into Ghost (*A* and *B*) and HeLa (*C* and *D*) cells. Confocal images of the CLND1-CD81 and CLDN1-LDLR BiFC complexes are shown. Antibody staining of EEA1 is shown in *red*. The *boxed areas* are magnified and shown in adjacent columns.

protein. To investigate whether Huh7 cells are capable of forming functional TJs (*i.e.* display proper localization of TJ-associated components and are able to restrict passive ion flow through the paracellular space), we co-stained the cells with ZO-1 (a well-known tight junction marker) and measured transepithelial electric resistance. We found that CLDN1 completely co-localized with ZO-1 at lateral cell-cell contacts which was identical to the staining pattern observed in the well-characterized polarized cell line Caco-2, which are known to form TJs (Fig. 6*A*). Ectopically expressed CLDN1 also co-localized with ZO-1 in GHOST and 293T cells at cell-cell contact sites but not in HeLa cells (Fig. 6*A*). Furthermore, in NIH3T3 cells, the endogenous levels of ZO-1 appeared to be low and a weak co-localization of ectopically expressed CLDN1 with endogenous ZO-1 was observed. However, the distribution of ZO-1 was rather different from what was seen in Huh7 cells in that ZO-1 distribution was discontinuous on cell-cell contact sites (Fig. 6*A*). Furthermore, when the transepithelial electric resistance was measured, Huh7 cells developed increasing resistances over a 6-day incubation period, consistent with what was observed for Caco-2 cells. In contrast, the resistance obtained from a HeLa-CLDN1 stable cell line remained constant during this period (Fig. 6*B*). As TER is a good indicator of the relative "tightness" of cells (*i.e.* TJ gating function), Huh7 cells clearly possess the characteristics of TJ-forming cell types.

Disruption of CLDN1 Localization Inhibits Viral Entry—If plasma membrane-bound or TJ-enriched CLDN1 is required for HCV entry, the disruption of CLDN1 localization is expected to abolish HCV entry. We tested this hypothesis by treating Huh 7.5.1 cells with TNF-α overnight. Cytokines such as IFN and TNF-α have been shown to disrupt TJs by inducing the internalization of TJ proteins in epithelial cells (32). As shown in Fig. 7*A*, plasma membrane-bound CLDN1 became internalized following TNF-α treatment. As a result, the infection of HCVpp in these cells decreased in a dose-dependent manner (Fig. 7*B*). In contrast, infection of VSVpp was not affected by TNF-α treatment (Fig. 7*B*). The same inhibitory effect could be repeated in TNF-α-treated Huh7.5.1 cells that were infected with JFH1 HCVcc as the production of the HCV core protein decreased in cells that were treated with TNF-α in a dose-dependent manner (Fig. 7*C*). As TNF-α was reported to neither affect HCV protein nor RNA synthesis (33), this inhibition is most likely due to the direct inhibition of HCVcc entry into TNF-α-treated cells. To ensure that this possibility is indeed the case, we infected cells with HCVcc prior to TNF-α treatment and found no effect on HCV core protein expression (Fig. 7*D*). Furthermore, the TNF-α doses used here did not cause any cell death as determined by morphological examination and trypan blue exclusion.

DISCUSSION

The exciting discovery of the TJ protein CLDN1 as a HCV co-receptor has provoked important questions: Does CLDN1 interact with HCV glycoproteins? What is the relationship between CLDN1 and other HCV co-receptors? Where is it localized? What role does CLDN1 play in HCV entry? The data presented in this study specifically address these questions and provide a better understanding of the role that CLDN1 might play in HCV entry.

Interactions between CLDN1 and HCV Glycoproteins and Co-receptors—To our knowledge, this is the first study to show that overexpressed CLDN1 co-precipitates with both HCV glycoproteins. This finding has provided the first piece of evidence that CLDN1 is biochemically capable of interacting with HCV

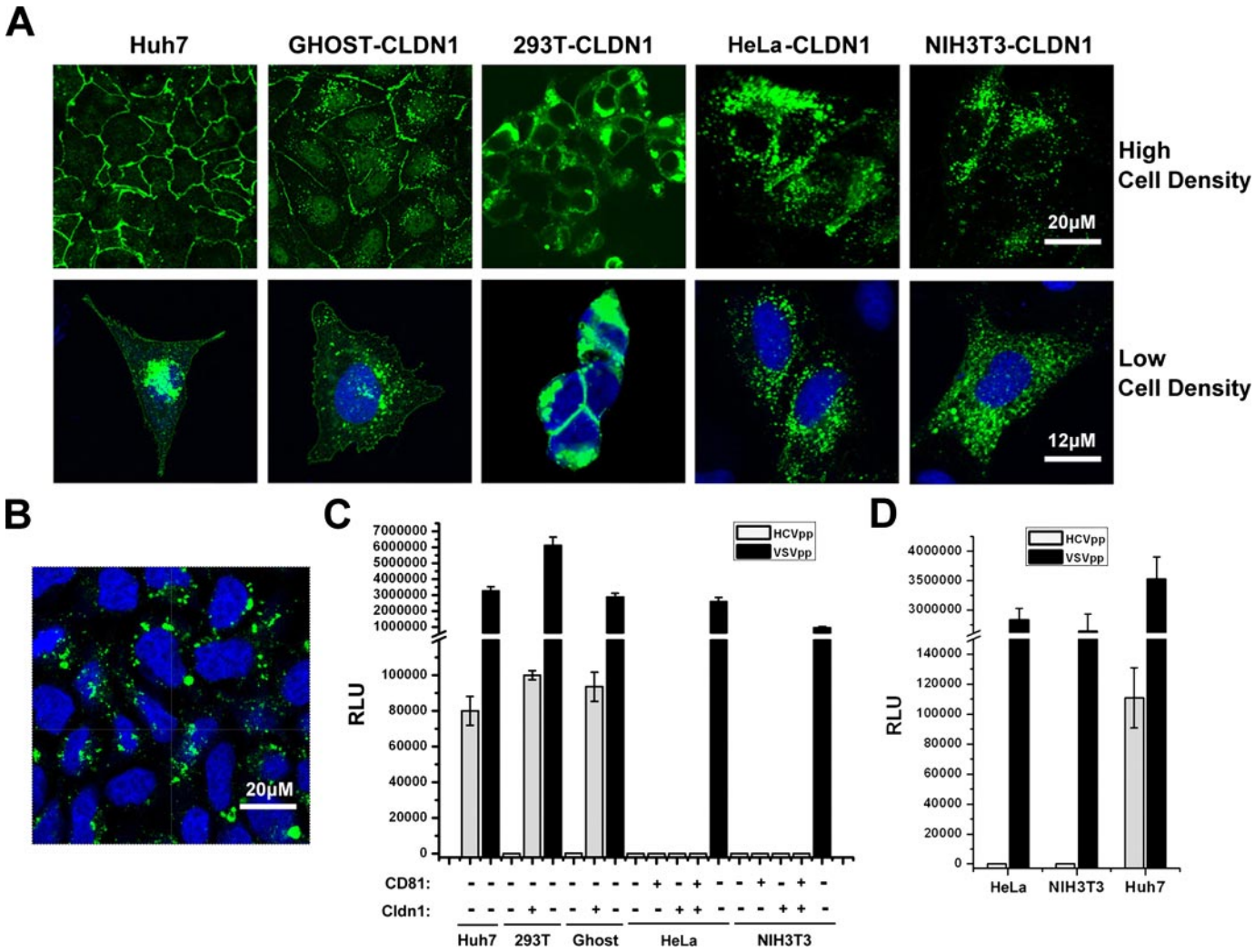

FIGURE 4. **Correlation of membrane distribution of CLDN1 with HCV permissiveness.** *A*, *upper panel*, confocal images were taken at high cell density to show endogenous CLDN1 in Huh7 cells and ectopically expressed CLDN1-GFP in indicated cell types. *Lower panel*, cells were transfected with the GFP-CLDN1 construct, and images were taken at low cell density. *B*, HeLa-CLDN1 stable cell line was stained for CLDN1 (*green signal*) and showed a scattered distribution in the cytoplasm. *C*, 293T, Ghost, HeLa, and NIH3T3 cells were transfected with the indicated plasmids and then infected with HCVpp (*gray bar*) or VSVpp (*black bar*) for an additional 2 days followed by luciferase assay. *D*, HeLa and NIH3T3 cells were each transfected with CLDN1-, CD81-, and LDLR-expressing constructs simultaneously. Twenty-four hours after transfection, cells were spin-inoculated with HCVpp (*gray bar*) or VSVpp virus (*black bar*) for 90 min and further incubated for 2 days followed by luciferase assay.

envelope proteins. Further studies are required to address whether CLDN1 comes into direct contact with virions during entry or whether CLDN1 plays an indirect role in virus entry. In fact, ectopically expressed CLDN1 and HCV E2 largely co-localized intracellularly in HeLa and Ghost cells, but not at the cell surface. This result could be explained by the findings that: 1) overexpressed proteins tend to have a large intracellular distribution; and 2) a specific conformation of the E1-E2 dimer is required for the surface interaction to occur and this confirmation is only found on an intact viral particle. To some extent, the overexpression system mimics what occurs during active viral replication when new viral proteins are synthesized. Consequently, it would be interesting to investigate whether newly synthesized HCV E1-E2 dimers interact with endogenous CLDN1 during viral infection and how that interaction might affect viral assembly and budding.

The BiFC assay offers unique features for the study of protein-protein interactions: 1) the results can be readily quantified; and 2) the assay allows for the simultaneous imaging of the location of an interaction. Using this approach, we were able to confirm the CLDN1-E1E2 interaction. Furthermore, we identified strong interactions between CLDN1, CD81, and LDLR. In support, a recent publication reported that CLDN1 co-precipitated with CD9 and CD81 and resided in tetraspanin-enriched membrane microdomains of lung epithelial cell lines (34). If CLDN1 acts at the later stage of viral entry as previously proposed (19), its interactions with CD81 and LDLR may occur only upon viral attachment. Ongoing experiments in our laboratory are targeted to addressing this issue by both biochemical approaches and co-localization studies of endogenous proteins.

Huh7 Cells Forms Tight Junctions—Perhaps the most intriguing question about CLDN1-mediated HCV entry is the following: Do cells require membrane localization of CLDN1 for entry? This question is of particular interest given that CLDN1 localizes to TJs in polarized hepatocytes. A recent study of Caco-2 cells showed that the disruption of TJ by calcium with-

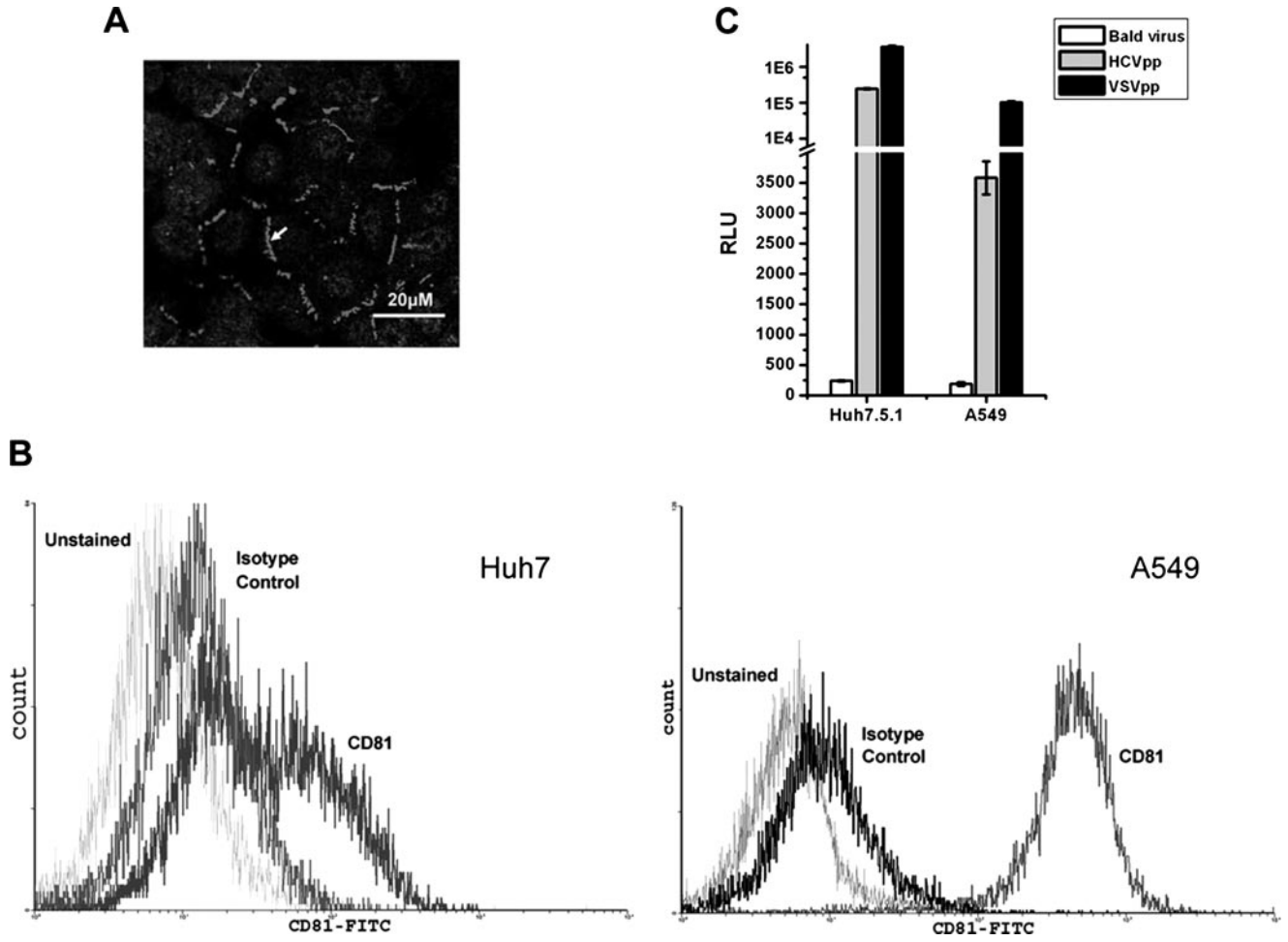

FIGURE 5. **Entry of HCVpp into the human lung cancer epithelial cell line A549.** *A*, confocal images of endogenous CLDN1 in A549 cells. The *white arrow* indicates CLDN1 enrichment at cell-cell contacts. *B*, surface expression of CD81 on A549 cells. A549 and Huh7 cells were stained with either anti-CD81 (JS-81, BD bioscience) (*green line*) or a control mouse IgG (*black line*) followed by FITC-secondary antibody staining. Positively stained cells were quantified using a Coulter XL flow cytometer. *Gray line*, unstained samples. *C*, 4×10^5 A549 cells were spin-inoculated with bald virus (*white bar*), HCVpp (*gray bar*), and VSVpp (*black bar*) followed by luciferase assay. HCVpp was able to infect A549 cells.

drawal increased HCV viral entry, implying that TJ-bound CLDN1 may not be essential for viral entry (31). Our results, however, at least support the idea that membrane-bound CLDN1 is required for HCV entry. Interestingly, among all permissive cell lines that we studied, CLDN1 appears to reside predominantly in either TJ or TJ-like structures and is co-localized with ZO-1. In particular, Huh7 cells form functional TJs as shown by confocal microscopy and transepithelial electric resistance measurements. This result is not surprising given that primary hepatocytes are highly polarized (35), a characteristic that is dependent upon the formation of tight junctions between adjacent cells.

We would like to emphasize that the cellular polarity of the widely used Huh7 cell line and its derivatives (Huh7.5, Huh 7.5.1), although highly permissive to HCVcc and HCVpp infection, remain to be determined. However, even non-polarized cells can form TJ-like structures (28). We have now shown that CLDN1 distribution in permissive cell lines is highly enriched at cell-cell contacts that resemble TJ-like structures. In addition, CLDN1 co-localizes with CD81 and LDLR on plasma membranes in permissive cells and the disruption of membrane-bound CLDN1 inhibits viral entry. Although the mechanism by which HCV accesses TJ-sequestered CLDN1 remains unknown, it is attractive to speculate that the virus may utilize a route similar to that taken by Group B Coxsackieviruses (CVBs), which access TJ-localized receptors via alternative receptor binding on the apical surface and relocalization to the junctional complex (36, 37). Further studies will be required to elucidate the route utilized by HCV to access CLND1 and the mechanistic role of CLDN1 in HCV entry.

Potential Role of CLDN1 in HCV Entry—CVB enters polarized epithelial cells from the TJ, causing a transient disruption of TJ integrity. During this process, CVB stimulates the specific internalization of occludin, a TJ-localized integral membrane component with structural similarities to CLDNs, within macropinosomes (29, 38). Interestingly, although CVBs do not directly bind occludin, occludin is required for a post-attachment step in virus entry. Cellular entry of enveloped HCV particles has been demonstrated to rely on clathrin-dependent endocytosis (11, 12). However, neither CD81 nor SR-BI, two of the known required HCV entry receptors, is actively endocytosed. On the other hand, CLDN1 and other TJ proteins have been shown to be actively recycled between endosomes and TJ via a clathrin-dependent endocytic mechanism (39). Treatment

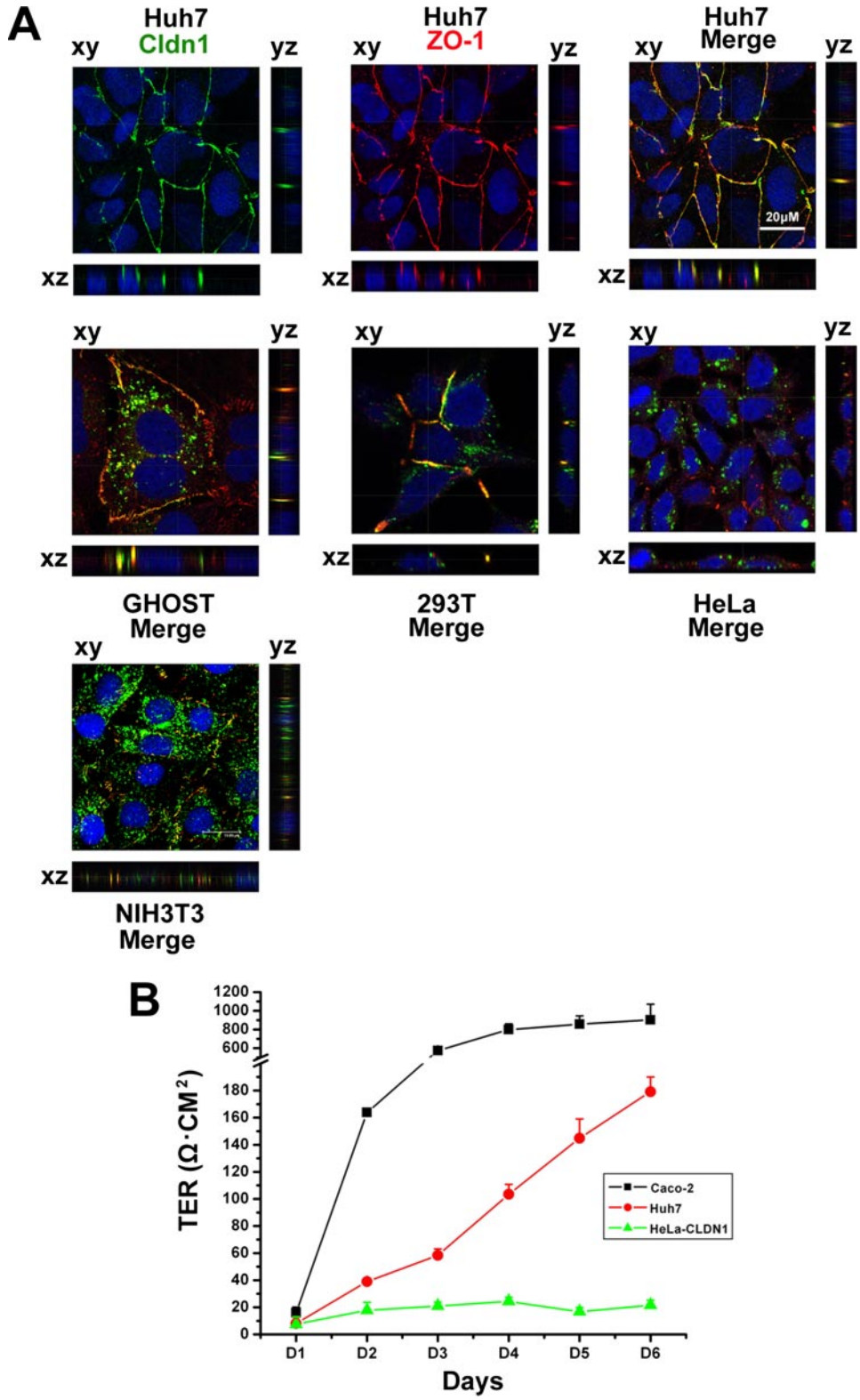

FIGURE 6. **Formation of tight junctions in Huh7 cells.** *A*, confluent Huh7 cells and stable cell lines derived from GHOST, 293T, HeLa, and NIH3T3 cells that express full-length CLDN1 were fixed and stained for CLDN1 (*green*) and ZO-1 (*red*). Single, colored, and merged images are presented for Huh7 cells; only merged images are shown for other cell types. Images were captured with a Leica TCS-SL confocal microscope. The *large panels* represent XY sections and the *small panels* represent YZ and XZ sections. XZ and YZ series sections were complied stacks acquired at 0.5-μM intervals. The *gray thin lines* in the XY sections indicate the planes where Z sections were taken. *Scale bar* represents 20 μm. *B*, 10^4 Huh7, Caco-2, and HeLa-CLDN1 cells were seeded in a 24-well transwell plate (6.5-mm membrane diameter, 0.4-μm pore size). The next day (*D1*), TER was measured and followed subsequently for 6 days. All cell types became confluent on day 2. Caco-2 cells grew just slightly faster than the rest two cell types. But only the TER of HeLa-CLDN1 cells remained unchanged throughout the course of the experiment. TER is plotted as ohms time area ($\Omega \cdot cm^2$).

of epithelial cells with either IFN-γ or TNF-α modulates epithelial permeability by inducing the internalization of several TJ proteins, including occludin, junction adhesion molecule A, and CLDN1 (32). Another CLDN family member, Claudin-3, was identified as the receptor for *Clostridium perfringens* enterotoxin (CPE). CPE induces CLDN3 endocytosis and increases paracellular permeability by binding to the second extracellular loop domain of Claudin-3 (40). It is conceivable that binding of the virions to CLDN1 may directly trigger CLDN1 internalization, facilitating viral entry. Consistent with this notion, CLDN1 forms a complex with CD81 on the plasma membrane as well as in the cytoplasm of Huh7, 293T-CLDN1, and GHOST-CLDN1 stable cell lines. The intracellular CLDN1-CD81 complex co-localizes with EEA1, an early endosomal marker. Perhaps HCV first attaches to host cells via CD81 or another unidentified cellular receptor(s) followed by the transfer of the virus to CLDN1-enriched regions. It may then become internalized into early endosomes where a low pH change triggers the fusion process, leading to the release of virus into the cytoplasm.

Alternatively, CLDN1 may serve as a membrane scaffold upon which other cellular HCV entry factors assemble to form an active entry complex, but does not undergo endocytosis itself. Evidence that supports this possibility comes from observations that CLDN1-mediated HCV entry is independent of the C-terminal domain to which PDZ-domain proteins bind (19). The interactions of CLDN1 with these proteins are likely to be important for its internalization. Furthermore, CLDN1 associates with CD81 and LDLR on the cell surface and is capable of binding to both HCV E1 and E2 proteins, thus increasing viral attachment (supplemental Fig. S4).

Regardless of how CLDN1 mediates HCV entry, we have identified a novel mechanism by which cellular

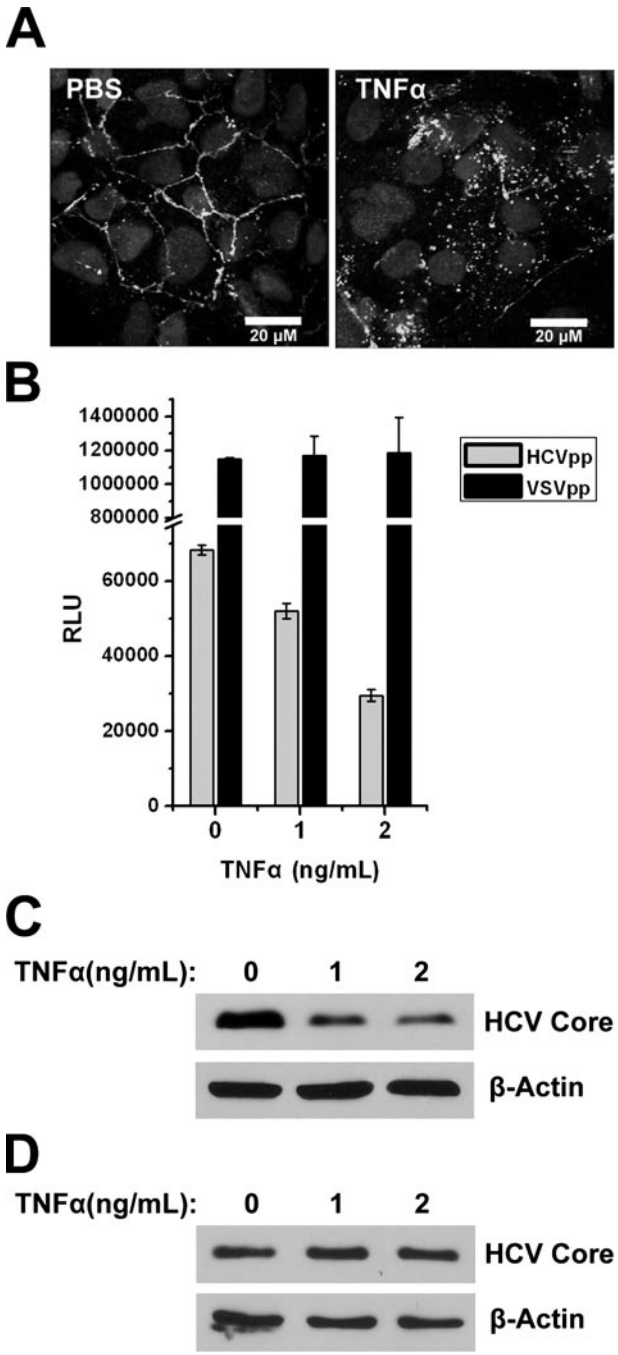

FIGURE 7. **Requirement of cell-cell contact-enriched CLDN1 for HCV entry.** *A*, TNF-α induced CLDN1 internalization in the liver cell line. Confluent Huh7.5.1 cells were treated with 1 ng/ml TNF-α or PBS overnight, followed by immunofluorescent staining of endogenous CLDN1 (*green*). *B*, Huh7.5.1 cells were treated with different dosages of TNF-α overnight and then infected with HCVpp (*gray bar*) or VSVpp (*black bar*) for luciferase assay. *C*, Huh7.5.1 cells were treated with different dosages of TNF-α overnight and then infected by HCVcc (multiplicity of infection = 0.1). Cells were lysed after 3 days, and Western analysis was carried out using anti-core and anti-β-actin antibodies. *D*, Huh7.5.1 cells were infected with HCVcc (multiplicity of infection = 0.1) overnight followed by an additional twenty-four hours of incubation to allow sufficient viral replication. Cells were then treated with TNF-α overnight and then lysed for Western analysis.

tropism of HCV is controlled. Different cell types may distribute CLDN1 differentially and thus control their susceptibility to HCV infection. In HeLa and NIH3T3 cells, ectopically expressed CLDN1 is retained in early endosomes, possibly due to the inability of CLDN1 to reach the cell surface or its failure to be retained on the surface. In fact, this finding is not unusual because differential CLDN1 subcellular distribution patterns have been reported previously (41, 42). Furthermore, the small GTPase Rab13 was shown to regulate the surface distribution of CLDN1 in non-polarized fibroblasts (43). Interestingly, Rab13 is distributed in cytoplasmic vesicles in non-polarized cells but co-localizes with the TJ marker, ZO-1, in polarized epithelial cells (44), implying that the localization of Rab13 is also under tight regulation. Nevertheless, CLDN1 distribution, and not merely its expression *per se*, may mediate viral entry. The fact that non-hepatic cell lines A549 and Caco-2 are readily infected by HCVpp implies that cell types that express CLDN1 on their surfaces along with other co-receptors may be permissive to HCV infection as well. It was proposed that HeLa cells were non-permissive to HCV infection because they lack the expression of an unidentified co-receptor (19). In contrast, our findings suggest that the lack of CLDN1 cell surface distribution may instead render these cells resistant to infection. Identifying factors that regulate CLDN1 trafficking will likely provide important clues that may uncover this mystery.

Acknowledgments—We thank Drs. C. Rice, F. Chisari, G. Luo, F. Cosset, J. Dubuisson, H. Greenberg, Q. Wang, and T. Wakita for providing cell lines, constructs, and antibodies. We are also very grateful to G. Papworth and J. Devlin for technical support with confocal microscopy. We would like to acknowledge Drs. K. Li, Yee, and Reinhart for critical reading of the manuscript.

REFERENCES

1. Diedrich, G. (2006) *FEBS J.* **273,** 3871–3885
2. Bartosch, B., Dubuisson, J., and Cosset, F. L. (2003) *J. Exp. Med.* **197,** 633–642
3. Cormier, E. G., Tsamis, F., Kajumo, F., Durso, R. J., Gardner, J. P., and Dragic, T. (2004) *Proc. Natl. Acad. Sci. U. S. A.* **101,** 7270–7274
4. Hsu, M., Zhang, J., Flint, M., Logvinoff, C., Cheng-Mayer, C., Rice, C. M., and McKeating, J. A. (2003) *Proc. Natl. Acad. Sci. U. S. A.* **100,** 7271–7276
5. Cocquerel, L., Meunier, J. C., Pillez, A., Wychowski, C., and Dubuisson, J. (1998) *J. Virol.* **72,** 2183–2191
6. Cocquerel, L., Duvet, S., Meunier, J. C., Pillez, A., Cacan, R., Wychowski, C., and Dubuisson, J. (1999) *J. Virol.* **73,** 2641–2649
7. Cocquerel, L., Wychowski, C., Minner, F., Penin, F., and Dubuisson, J. (2000) *J. Virol.* **74,** 3623–3633
8. Cocquerel, L., Voisset, C., and Dubuisson, J. (2006) *J. Gen. Virol.* **87,** 1075–1084
9. Bartosch, B., and Cosset, F. L. (2006) *Virology* **348,** 1–12
10. Codran, A., Royer, C., Jaeck, D., Bastien-Valle, M., Baumert, T. F., Kieny, M. P., Pereira, C. A., and Martin, J. P. (2006) *J. Gen. Virol.* **87,** 2583–2593
11. Blanchard, E., Belouzard, S., Goueslain, L., Wakita, T., Dubuisson, J., Wychowski, C., and Rouille, Y. (2006) *J. Virol.* **80,** 6964–6972
12. Meertens, L., Bertaux, C., and Dragic, T. (2006) *J. Virol.* **80,** 11571–11578
13. Pileri, P., Uematsu, Y., Campagnoli, S., Galli, G., Falugi, F., Petracca, R., Weiner, A. J., Houghton, M., Rosa, D., Grandi, G., and Abrignani, S. (1998) *Science* **282,** 938–941
14. Scarselli, E., Ansuini, H., Cerino, R., Roccasecca, R. M., Acali, S., Filocamo, G., Traboni, C., Nicosia, A., Cortese, R., and Vitelli, A. (2002) *EMBO J.* **21,** 5017–5025
15. Petracca, R., Falugi, F., Galli, G., Norais, N., Rosa, D., Campagnoli, S., Burgio, V., Di Stasio, E., Giardina, B., Houghton, M., Abrignani, S., and Grandi, G. (2000) *J. Virol.* **74,** 4824–4830
16. Zhang, J., Randall, G., Higginbottom, A., Monk, P., Rice, C. M., and McKeating, J. A. (2004) *J. Virol.* **78,** 1448–1455

17. Lindenbach, B. D., Evans, M. J., Syder, A. J., Wolk, B., Tellinghuisen, T. L., Liu, C. C., Maruyama, T., Hynes, R. O., Burton, D. R., McKeating, J. A., and Rice, C. M. (2005) *Science* **309,** 623–626
18. Kato, T., Date, T., Miyamoto, M., Zhao, Z., Mizokami, M., and Wakita, T. (2005) *J. Virol.* **79,** 592–596
19. Evans, M. J., von Hahn, T., Tscherne, D. M., Syder, A. J., Panis, M., Wolk, B., Hatziioannou, T., McKeating, J. A., Bieniasz, P. D., and Rice, C. M. (2007) *Nature* **446,** 801–805
20. Van Itallie, C. M., and Anderson, J. M. (2004) *Physiology (Bethesda)* **19,** 331–338
21. Schneeberger, E. E., and Lynch, R. D. (2004) *Am. J. Physiol. Cell Physiol.* **286,** C1213–C1228
22. Cai, Z., Zhang, C., Chang, K. S., Jiang, J., Ahn, B. C., Wakita, T., Liang, T. J., and Luo, G. (2005) *J. Virol.* **79,** 13963–13973
23. Zhong, J., Gastaminza, P., Cheng, G., Kapadia, S., Kato, T., Burton, D. R., Wieland, S. F., Uprichard, S. L., Wakita, T., and Chisari, F. V. (2005) *Proc. Natl. Acad. Sci. U. S. A.* **102,** 9294–9299
24. Shyu, Y. J., Liu, H., Deng, X., and Hu, C. D. (2006) *BioTechniques* **40,** 61–66
25. Op De Beeck, A., Montserret, R., Duvet, S., Cocquerel, L., Cacan, R., Barberot, B., Le Maire, M., Penin, F., and Dubuisson, J. (2000) *J. Biol. Chem.* **275,** 31428–31437
26. Cocquerel, L., Kuo, C. C., Dubuisson, J., and Levy, S. (2003) *J. Virol.* **77,** 10677–10683
27. Jin, J., Sturgeon, T., Chen, C., Watkins, S. C., Weisz, O. A., and Montelaro, R. C. (2007) *J. Virol.* **81,** 11226–11235
28. Furuse, M., Fujita, K., Hiiragi, T., Fujimoto, K., and Tsukita, S. (1998) *J. Cell Biol.* **141,** 1539–1550
29. Coyne, C. B., and Bergelson, J. M. (2006) *Cell* **124,** 119–131
30. Hrzenjak, A., Reicher, H., Wintersperger, A., Steinecker-Frohnwieser, B., Sedlmayr, P., Schmidt, H., Nakamura, T., Malle, E., and Sattler, W. (2004) *Cell Mol. Life Sci.* **61,** 1520–1531
31. Mee, C. J., Grove, J., Harris, H. J., Hu, K., Balfe, P., and McKeating, J. A. (2008) *J. Virol.* **82,** 461–470
32. Bruewer, M., Utech, M., Ivanov, A. I., Hopkins, A. M., Parkos, C. A., and Nusrat, A. (2005) *Faseb. J.* **19,** 923–933
33. Frese, M., Barth, K., Kaul, A., Lohmann, V., Schwarzle, V., and Bartenschlager, R. (2003) *J. Gen. Virol.* **84,** 1253–1259
34. Kovalenko, O. V., Yang, X. H., and Hemler, M. E. (2007) *Mol. Cell. Proteomics.* **6,** 1855–1867
35. Silver, D. L., Wang, N., Xiao, X., and Tall, A. R. (2001) *J. Biol. Chem.* **276,** 25287–25293
36. Walters, R. W., Freimuth, P., Moninger, T. O., Ganske, I., Zabner, J., and Welsh, M. J. (2002) *Cell* **110,** 789–799
37. Bergelson, J. M., Cunningham, J. A., Droguett, G., Kurt-Jones, E. A., Krithivas, A., Hong, J. S., Horwitz, M. S., Crowell, R. L., and Finberg, R. W. (1997) *Science* **275,** 1320–1323
38. Carolyn B. Coyne, L. S., Jerrold R. Turner, and Jeffrey M. Bergelson. (2007) *Cell Host Microbe* **2,** 181–192
39. Ivanov, A. I., Nusrat, A., and Parkos, C. A. (2004) *Mol. Biol. Cell* **15,** 176–188
40. Fujita, K., Katahira, J., Horiguchi, Y., Sonoda, N., Furuse, M., and Tsukita, S. (2000) *FEBS Lett.* **476,** 258–261
41. Dhawan, P., Singh, A. B., Deane, N. G., No, Y., Shiou, S. R., Schmidt, C., Neff, J., Washington, M. K., and Beauchamp, R. D. (2005) *J. Clin. Investig.* **115,** 1765–1776
42. Gregory, M., Dufresne, J., Hermo, L., and Cyr, D. (2001) *Endocrinology* **142,** 854–863
43. Yamamoto, Y., Nishimura, N., Morimoto, S., Kitamura, H., Manabe, S., Kanayama, H. O., Kagawa, S., and Sasaki, T. (2003) *Biochem. Biophys. Res. Commun.* **308,** 270–275
44. Zahraoui, A., Joberty, G., Arpin, M., Fontaine, J. J., Hellio, R., Tavitian, A., and Louvard, D. (1994) *J. Cell Biol.* **124,** 101–115